Chemical Physics 425 (2013) 126–133

Contents lists available at ScienceDirect

Chemical Physics

journal homepage: www.elsevier.com/locate/chemphys

On the theoretical description of nuclear quadrupole coupling in Π states of small molecules

J. Fišer [a], R. Polák [b,*]

[a] Department of Physical and Macromolecular Chemistry, Faculty of Science, Charles University in Prague, Hlavova 2030, 128 40 Prague 2, Czech Republic
[b] J. Heyrovský Institute of Physical Chemistry, Academy of Sciences of the Czech Republic, v.v.i, Dolejškova 3, 182 23 Prague 8, Czech Republic

ARTICLE INFO

Article history:
Received 28 June 2013
In final form 13 August 2013
Available online 30 August 2013

Keywords:
Π States
Nuclear quadrupole coupling constant
Electric dipole moment
Diatomic spectroscopic constant

ABSTRACT

Axial (eQq_0) and perpendicular (eQq_2) nuclear quadrupole coupling constants were evaluated from the electric field gradient at the quadrupolar nuclei (^{7}Li, ^{14}N, ^{17}O, ^{33}S, ^{35}Cl) in diatomic (LiO, CN, NH^+, NH, N_2^+, NO, OH, HCl^+, CCl, OCl, NS) and polyatomic (C_2N, C_4N, NCO, N_3) Π states. For diatomics the nuclear quadrupole coupling constants (NQCCs) were determined as a function of the vibrational quantum number. The calculations were performed using the internally contracted multireference configuration interaction and single-configuration coupled-cluster approaches with large correlation-consistent basis sets. The overall quality of the wave functions was tested by comparing the calculated electric dipole moments and diatomic spectroscopic constants with external data. The calculated NQCCs were discussed and compared with previous experimental and theoretical studies.

1. Introduction

For linear molecules in electronic Σ states there is a considerable body of literature on the calculation of nuclear quadrupole coupling constants (NQCCs), helping to explain the hyperfine structure in molecular microwave spectra arising from interactions of the molecular fields with nuclear electric and/or magnetic moments. For such a molecule with the molecular axis chosen as axis z, possessing one nucleus A with nonzero effective electric quadrupole moment Q_A, the first-order perturbation energy values for nuclear quadrupole coupling can be expressed in the form [1]

$$E_Q = -eQ_A qY(I,J,F), \tag{1}$$

where e is the elementary electric charge, Y is a function (part of which is the Casimir function) of quantum numbers of nuclear spin (I), angular momentum associated with molecular rotation (J) and total angular momentum (F). Y is common to all molecules satisfying the above given space symmetry definition. q stands for the component of the Born–Oppenheimer electric field gradient tensor (EFG), $q = q_{zz} = \partial^2 V/\partial z^2$ (V being the electrostatic potential at the nucleus A), fulfilling $q_{zz} = -2q_{xx} = -2q_{yy}$ because of the cylindrical symmetry of the molecule. The product eQ_Aq is called the nuclear quadrupole coupling constant for the nucleus A in the molecule. The "molecular" value of Q_A has been in many cases successfully determined by combining the experimental data for NQCC and the precisely calculated EFG at the nucleus A in a small (preferably diatomic) molecule [2]. Of course, for heavy elements relativistic effects have to be taken into account [3,4].

Far less attention in the past has been devoted to the description of the nuclear quadrupole coupling in linear molecules with a spatially degenerate electronic state, particularly to the impact of axially asymmetric charge distribution on electric tensorial properties (see for instance Refs. [5,6]). The degenerate electronic states provide nonzero projections Λ of the total orbital angular momentum onto the molecular axis, exhibiting additional splitting of energy levels due to the electron and orbital angular momentum interactions. Consequently, two NQCCs have to be introduced reflecting both the cylindrically and noncylindrically symmetric charge distribution around the molecular axis [7–9]. Western et al. [10] defined the nitrogen nuclear quadrupole coupling in the ^{2}Π state of NO by means of an electron localized in a doubly degenerate π orbital $|\Lambda = \pm 1\rangle$ (Λ being the quantum number determining the component of angular momentum along the bond axis) as

$$eQ_N q_0 = eQ_N \left\langle \Lambda = \pm 1 \left| \sum \frac{e_i}{r_i^3} (3\cos^2\theta_{iz} - 1) \right| \Lambda = \pm 1 \right\rangle, \tag{2a}$$

$$eQ_N q_2 = eQ_N \left\langle \Lambda = \pm 1 \left| \sum \frac{e_i}{r_i^3} 3\sin^2\theta_{iz} \exp(\pm 2i\phi_{iz}) \right| \Lambda = \mp 1 \right\rangle, \tag{2b}$$

where the sum runs over all charged particles in the molecule except the nitrogen nucleus. By transforming the complex states $\Lambda = \pm 1$ to real π_x and π_y orbitals, Western et al. [10] arrived at the expressions

* Corresponding author. Tel.: +420 2 6605 2077; fax: +420 2 8658 2307.
E-mail address: rudolf.polak@jh-inst.cas.cz (R. Polák).

0301-0104/$ - see front matter © 2013 Elsevier B.V. All rights reserved.
http://dx.doi.org/10.1016/j.chemphys.2013.08.007

$$eQ_N q_0 = eQ_N q_{zz}, \tag{3a}$$

$$eQ_N q_2 = 2eQ_N(q_{yy} - q_{xx}). \tag{3b}$$

Analogous formulae were later on applied [6,11,12] to the evaluation of nuclear quadrupole coupling by using higher levels of approximation based on multireference configuration interaction, coupled cluster and density functional approaches. The term (3b) resembles the asymmetric parameter η [1] used to specify the quadrupole coupling of asymmetric top molecules in taking into account the departure of the field gradient from cylindrical symmetry about the reference axis.

Given the possibility of calculating $eQ_A q_0$ and $eQ_A q_2$ using the generalized Eqs. (3a) and (3b), we applied these formulae to obtain an overview about the reliability of predicting NQCCs in Π states for a series of linear molecules consisting of twelve diatomic, three triatomic and one five-atomic species containing one of the quadrupolar atoms: ^{7}Li, ^{17}O, ^{35}Cl or ^{14}N. To assess the accuracy of this approach we gathered together primarily references for the experimental quadrupole coupling parameters. Such values are missing only for systems (N_2^+, N_3) with more than one coupling nucleus where the determination of the NQCCs from experimental data is difficult due to the complex quadrupole interaction. Because different conventions can affect the sign of the perpendicular quadrupole coupling constants in the standard effective hyperfine Hamiltonian, in our numerical results we recommend to pay attention preferentially to the magnitude of these parameters. Since only molecules containing relatively light quadrupolar atoms were dealt with, no relativistic effects were included into the calculation of the EFGs.

2. Computational details

The calculation of potential energy E, Born–Oppenheimer EFG tensor at the nucleus A, $\boldsymbol{q}$, and the electric dipole moment μ has been carried out using the following methods: the CASSCF/icMRCI (complete-active space SCF followed by an internally contracted multireference configuration interaction) method [13–16] using the MOLPRO (version 2010.1) suite of programs [17], and the CCSD(T) (single-configuration coupled-cluster approach including single, double and a perturbative estimate of triple excitations) method [18–21] with restricted open-shell Hartree–Fock (ROHF) orbitals employing the local version of ACES II [22] electronic structure program package. The latter method for calculating first-order properties by means of the finite field approach was systematically applied at the all-electron level to the whole collection of investigated systems. The multi-configuration self-consistent icMRCI calculations, together with the coupled-cluster T_1 diagnostic [23,24], were used for assessing the appropriateness of the single-reference approximation in the CCSD(T) computations. The coupled cluster method with frozen core (fc) approximation (version RCCSD(T) in MOLPRO implementation, correlating solely valence electrons) was used for selected comparative purposes and for geometry optimization. In all our earlier calculations of EFGs we found that both the expectation value method and the finite field approximation [25–27] lead to close results (e.g. [28–30]) compared to effects caused by the choice of basis set, deviations in equilibrium geometry etc.

According to the size of a molecule, several correlation-consistent polarized valence (cc-pVXZ, X = T,Q,5) basis sets of Dunning and coworkers, including augmented (aug) and core-valence (CV) versions [31–33] were used. Particularly for diatomic systems within the icMRCI calculations, cc-pCV5Z and aug-cc-pV5Z basis sets were assigned to the quadrupolar atom and the other atom, respectively, with the exception of OH ($X^2\Pi$): Because the icMRCI procedure with the quintuple basis did not converge, the cc-pCVQZ together with aug-cc-pVQZ basis set were used instead. For similar reasons, in the coupled cluster calculations of OH, the cc-pCV5Z basis set was used for both atoms. For systems with a larger number of electrons (C_4N and diatomics containing Cl atoms), smaller basis sets had to be applied because of computer memory limitations. Without guaranteeing the optimum choice in general, such a type of basis set in conjunction with appropriate many-electron methods has been found sufficiently reliable [34,35] for calculating EFGs at atomic nuclei.

Concerning the CASSCF calculations, various types of active spaces (ASs) were used. Calculations on diatomics were performed at the AS comprising valence and core (i.e. 1s-like) orbitals. Thus, diatomics consisting of first and second row atoms were described by 10 active orbitals 1σ–6σ, 1π, 2π, ordered as $(6\times a_1, 2\times b_1, 2\times b_2, 0\times a_2) \equiv (6,2,2,0)$ in C_{2v} symmetry, allowing to treat core correlation phenomena. The ASs serving to the description of CCl and NS were extended by the orbitals 7σ, 8σ, 3π, 4π, rising the dimension of the active space to 14. A different AS, namely (9,4,4,0) with the orbitals 1σ–3σ and 1π closed, was used to obtain optimum values for the components of the EFG at the nucleus Cl in OCl, in competition with the ASs (8,3,3,0) and (9,3,3,0) including inner 1s orbitals. In treating the three atomic systems in Table 3, the "standard" full valence AS was used. The respective dimensionality n_{AS} of the AS, together with the number n_e of active electrons referring to individual calculations, are presented in Tables 1 and 2 in short-hand notation as (n_e, n_{AS}).

Effective electric quadrupole moments of nuclei of selected isotopes appearing in our calculations were taken from Ref. [2]: $Q(^7\text{Li}) = -0.0401$ b, $Q(^{17}\text{O}) = -0.02558$ b, $Q(^{35}\text{Cl}) = -0.08165$ b, $Q(^{33}\text{S}) = -0.0678$ b and $Q(^{14}\text{N}) = 0.02044$ b.

In order to confirm the quality of the basis sets and the methods used in this investigation, and to aid comparison with previous work on given systems, besides the EFGs also the electric dipole moments were calculated, and spectroscopic constants for diatomic species were derived numerically from the potential energy functions (PEFs) using the subroutine VIBROT, a component of the MOLCAS-4 suite of *ab initio* programs [36]. This package of programs was also applied to the vibrational averaging of the electric field gradient values q_0 and q_2 in diatomic molecules. Rotational averaging of these quantities in similar molecules was found in our earlier studies [28,29] to be negligible.

3. Results a discussion

Table 1 lists the calculated NQCCs at the equilibrium internuclear distance R_e, and for four lowest vibrational states of selected diatomic molecules in their Π-electronic states. Further, the coupling constants are compared with existing experimental and previously obtained theoretical values. Our theoretical NQCCs were derived from the EFG curves $q(R)$ and PEFs $E(R)$, the latter ones characterized by the set of spectroscopic constants displayed in Table 2. It should be emphasized that the choice of the basis sets favors the calculation of the electric field gradient in comparison with other physical quantities. By way of illustration, the input data leading to the vibrationally dependent NQCCs for the Π states of NH and NH^+ are shown in Fig. 1.

The results summarized in Table 1 show that there are no marked differences in the NQCC values corresponding to R_e and the vibrational $v = 0$ state, with the exception of eQq_0 at ^{14}N in the NH ($c^1\Pi$) state where the difference reaches almost 10 % of the coupling constant. Further, the icMRCI coupling constants are closely similar to the CCSD(T) results, showing alike tendencies in deviations from the experimental data.

First of all it is appropriate to compare our results with other available theoretical data. For six diatomic species in the 12-mem-

Table 1
NQCCs (eQq_i, i = 0, 2) (in MHz) for four lowest vibrational states in selected Π-electronic states of diatomic molecules calculated at own optimized geometry (cf. Table 2) and compared with external data.

Species	Nucleus	Method	i	$(eQq_i)_e$	eQq_{iv}			
					v = 0	v = 1	v = 2	v = 3
LiO ($X^2\Pi$)	^{7}Li	CASSCF(11,10)/icMRCI/CA5[a]	0	0.450	0.445	0.438	0.431	0.425
			2	0.307	0.304	0.295	0.286	0.278
		CCSD(T)/CA5	0	0.445	0.441	0.432	0.424	0.416
			2	0.333	0.330	0.322	0.315	0.309
		Radio-frequency spectry [8]	0		0.444(8)			
			2		0.109(18)			
		Microwave spectry [37]	0		0.463(20)	0.476(50)		
		B3LYP/aug-cc-pVQZ [6][b]	0	0.56				
			2	0.43				
CN ($A^2\Pi$)	^{14}N	CASSCF(13,10)/icMRCI/CA5	0	-6.409	−6.367	−6.283	−6.201	−6.109
			2	-17.390	−17.345	−17.312	−17.279	−17.215
		CCSD(T)/CA5	0	-6.349	−6.305	−6.228	−6.169	−6.056
			2	-17.305	−17.257	−17.230	−17.238	−17.121
		Sub-Doppler laser absorption spectry [39]	0		−5.71(49)			
			2		14.5(31)			
NH^+ ($X^2\Pi$)	^{14}N	CASSCF(7,10)/icMRCI/CA5	0	-10.859	−10.801	−10.759	−10.727	−10.699
			2	37.822	37.845	38.196	38.553	38.905
		CCSD(T)/CA5	0	-10.896	−10.840	−10.768	−10.710	−10.665
			2	37.844	37.864	38.052	38.242	38.430
		Laser sideband technique [40]	0		−9.6(65)			
			2		−37.2(98)			
		Laser magnetic resonance [41]	0		−9.6(23)			
			2		34.7(34)			
NH ($A^3\Pi$)	^{14}N	CASSCF(8,10)/icMRCI/CA5	0	7.251	7.406	7.779	8.176	8.624
			2	-26.610	−26.628	−26.780	−26.948	−27.140
		CCSD(T)/CA5	0	7.245	7.404	7.798	8.236	8.723
			2	-26.424	−26.438	−26.601	−26.776	−26.956
		Laser-induced spectry [9]	0		7.1(15)			
			2		21.9(24)			
		B3LYP/aug-cc-pVQZ [6][b]	0	7.780				
			2	28.37				
NH ($c^1\Pi$)	^{14}N	CASSCF(8,10)/icMRCI/CA5	0	8.310	9.082	9.760	10.699	11.651
			2	-29.287	−29.000	−28.947	−28.640	−27.502
		Laser-induced spectry [42]	0		11.4(23)			
			2		−32.0(32)			
N_2^+ ($A^2\Pi_u$)	^{14}N	CASSCF(13,10)/icMRCI/aug-cc-pCV5Z	0	-7.423	−7.372	−7.293	−7.224	−7.117
			2	-17.198	−17.202	−17.403	−17.632	−17.780
		CCSD(T)/cc-pCV5Z	0	-7.417	−7.369	−7.282	−7.201	−7.102
			2	-17.178	−17.183	−17.270	−17.372	−17.441
		B3LYP/aug-cc-pVQZ [43][c]	0	8.11	7.97	7.83	7.68	7.59
			2	18.11	18.06	18.06	18.06	18.06
NO ($X^2\Pi$)	^{14}N	CASSCF(15,10)/icMRCI/CA5	0	-1.860	−1.821	−1.730	−1.640	−1.545
			2	23.233	23.173	23.142	23.105	23.031
		CCSD(T)/CA5	0	-1.935	−1.899	−1.821	−1.752	−1.657
			2	23.197	23.157	23.195	23.274	23.182
		IR-radiofr. double resonance spectry [44]	0		−1.8565(3)	−1.78(3)		
			2		23.158(6)	23.0(1)		
		Pure rotational spectry [45]	0		−1.85749(74)			
			2		23.049(18)			
		B3LYP/aug-cc-pVQZ [6][b]	0	-2.30				
			2	26.0				
OH ($X^2\Pi$)	^{17}O	CASSCF(9,10)/icMRCI/CAQ	0	-1.478	−1.702	−2.218	−2.742	−3.277
			2	59.253	59.291	59.889	60.509	61.138
		CCSD(T)/cc-pCV5Z	0	-1.505	−1.719	−2.165	−2.572	−2.975
			2	59.022	59.059	59.428	59.809	60.228
		Far-IR laser magnetic res. spectry [46]	0		−1.92			
			2		66(9)			
		B3LYP/aug-cc-pVQZ [6][b]	0	-1.69				
			2	61.86				
HCl^+ ($X^2\Pi$)	^{35}Cl	CASSCF(9,10)[d]/icMRCI/CA5	0	-15.875	−16.170	−16.968	−17.813	−18.559
			2	322.342	332.275	324.740	326.935	329.229
		CASSCF(17,11)[e]/icMRCI/CA5	0	-13.923	−14.318	−15.417	−16.456	−17.463
			2	366.292	366.277	369.263	372.309	375.289
		CCSD(T)/CAQ	0	-12.590	−12.871	−13.522	−14.094	−14.604
			2	357.164	357.080	358.285	359.526	360.648
		Microwave spectry [47]	0		−7.8(83)			
			2		−143(25)			

Table 1 (*continued*)

Species	Nucleus	Method	i	$(eQq_i)_e$	eQq_{iv}			
					$v = 0$	$v = 1$	$v = 2$	$v = 3$
		Microwave spectry [48]	0		−8.03(210)			
			2		−364.9(188)			
		Median of DFT and *ab initio* results [49][f]	0	-12.5(4)				
			2	-169(1)				
CCl ($X^2\Pi$)	^{35}Cl	CASSCF(23,14)/icMRCI/CA5	0	-35.565	−35.749	−36.495	−37.239	−37.993
			2	-76.468	−76.051	−75.292	−74.562	−73.788
		CCSD(T)/CAQ	0	-33.435	−33.632	−34.288	−34.978	−35.751
			2	-76.116	−75.739	−75.114	−74.509	−73.814
		Microwave spectry [50]	0		−34.26(13)			
			2		84.6(95)			
OCl ($X^2\Pi$)	^{35}Cl	CASSCF(15,12)/icMRCI/CA5	0	-85.582	−85.942	−87.546	−89.152	−90.742
			2	112.322	111.151	108.603	106.073	103.494
		CCSD(T)/CAQ	0	-86.110	−84.668	−86.141	−88.019	−89.132
			2	119.098	121.666	118.101	114.189	111.832
		Mm and microwave spectry [51]	0		−87.95(19)	−88.48(46)		
			2		126.4(65)	126.4[g]		
		Submm spectry [52]	0		−88.020(83)			
			2		−116.0(56)			
NS ($X^2\Pi$)	^{14}N	CASSCF(23,14)/icMRCI/CA5	0	-3.035	−2.998	−2.909	−2.820	−2.727
			2	18.280	18.223	18.217	18.194	18.143
		CCSD(T)/CA5	0	-2.859	−2.828	−2.760	−2.693	−2.623
			2	17.475	17.437	17.403	17.362	17.299
		Mm-wave spectry [53]	0		−2.530(44)			
		Microwave spectry [54]	0		−2.515(30)			
			2		−3.30(151)			
		Mm-wave spectry [55]	0		−0.678(36)	−0.664(57)		
			2		−5.8(33)	−6.0(36)		

[a] CAX stands for the basis set including cc-pCVXZ and aug-cc-pVXZ (X = Q,5) sets assigned to the quadrupolar atom and the other atom, respectively.
[b] Derived from the q_{ii} values calculated at experimental R_e[38], the magnitude of eQq_2 is given.
[c] The magnitude of NQCCs is given.
[d] Definition of the orbital space for MCSCF: occupied (8,3,3,0), closed (2,1,1,0) in C_{2v} symmetry.
[e] Definition of the orbital space for MCSCF: occupied (7,2,2,0), closed (0).
[f] Calculated at experimental R_e (cf. Table 2).
[g] Fixed value.

ber collection, electric field gradient parameters q_{zz} and $|(q_{xx} - q_{yy})|$ were computed [6,43] by means of the density functional theory (DFT) at the B3LYP/aug-cc-pVQZ level with the exception of HCl^+[49] for which the data were expressed as medians of DFT and spin-unrestricted *ab initio* calculations. Except for HCl^+, the DFT NQCCs presented in Table 1 were acquired from the EFG parameters of Bruna and Grein [6,43] by using Eqs. (3a) and (3b), of course, without the possibility of ascribing a sign to eQ_Aq_2. Table 1 shows that all theoretical results exhibit deviations from the experimental ones in the same direction and of about the same magnitude. In three cases, LiO, NO and HCl^+, the icMRCI and CCSD(T) methods yield for the coupling constants somewhat closer values to the experimental ones than the DFT method; particularly $eQ_{Cl}q_2$ in HCl^+ comes out significantly closer to the coupling constant recently determined from the rotational spectrum of the species [48]. For the $A^2\Pi_u$ state of N_2^+ the experimentally determined hyperfine constants are unknown. With DFT [43] the magnitude of eQ_Nq_0 and eQ_Nq_2 come out by about 8% and 5% larger than with the CI and coupled cluster methods, and the R variations of the quadrupole coupling constants remain qualitatively similar: this can be considered as an acceptable agreement between both theoretical approaches.

With regard to the imine radical, NH, the calculated hyperfine parameters for the two low-lying Π states are seen to be in good agreement with the earlier observed parameters [9,42]. Both MRCI states, $A^3\Pi$ and $c^1\Pi$, which are dominated by the same MO configuration $..(3\sigma)^1(\pi)^3$ with a very similar reference coefficient $c_0 \sim 0.97$ and 0.96, respectively. This fact speaks in favor of the appropriateness of the spectroscopic approximation [7,9,42] used earlier to the qualitative explanation of the relationship between hyperfine parameters of the two electronic states. An even better agreement of the theoretical NQCCs with the previous experimental results of Hübers et al. [41] holds for the NH^+ $X^2\Pi$ state characterized by the $..(3\sigma)^2(\pi)^1$ leading configuration. Such compliance is somewhat astonishing in view of the fact that the electronic ground state of NH^+ is supposed to be in strong spin–orbit interaction with the $a^4\Sigma^-$ state.

The results in Table 1 concerning the $A^2\Pi$ state of CN complement the theoretical ^{14}N NQCC data for low-lying Σ electronic states in CN^+, CN and CN^- reported earlier [28,62,63]. The two theoretical quadrupole coupling parameters of the Π state agree well with the constants derived from sub-Doppler laser absorption spectroscopy measurements [39]. Further, the highly dominant $..(5\sigma)^2(\pi)^3$ electron configuration (with c_0~0.94) in the MRCI wave function corroborates the qualitative orbital characterization used for the interpretation of the quadrupole coupling constants [39]. The agreement between experiment and theory holds also for the insignificant vibrational dependence of the electric hyperfine interaction.

A rigorous comparison of computed vibrationally dependent NQCCs with experiment turns out difficult, as in most cases no experimental values are available. Within the selected diatomics, we found literature values only for four molecules, LiO (^{7}Li), NO and NS (^{14}N), and OCl (^{35}Cl), for which at least one of the two quadrupole coupling constants was experimentally determined for two lowest vibrational states.

For the LiO ($X^2\Pi$) radical with a large ionic character of the bond, there is good agreement between our theoretical and the experimental $eQ_{Li}q_0$ values [8,37], and the vibrational dependence of the theoretical values is within the limits of experimental error. However, there is marked difference in the magnitude of the non-diagonal $eQ_{Li}q_2$ parameter: The experimental value was deter-

Table 2
Comparison of calculated spectroscopic constants of selected Π-electronic states with experimental values (values taken from original literature are rounded to four decimal places).

Species	Method and basis set	R_e (Å)	ω_e (cm^{-1})	$\omega_e x_e$ (cm^{-1})	B_e (cm^{-1})	$\alpha_e \times 10^2$ (cm^{-1})	μ (D)
LiO ($X^2\Pi$)	MRCI/CA5[a]	1.688	817.0	8.19	1.212	1.80	6.659
	MRCI + Q	1.689	815.3	8.24	1.212	1.80	
	CCSD(T)/CA5	1.688	818.3	9.94	1.215	2.09	6.615
	Experiment [37]	1.6882	813.48(26)		1.2128	1.790	6.84(3)[b]
CN ($A^2\Pi$)	MRCI/CA5	1.233	1822.3	14.05	1.716	1.71	0.152
	MRCI + Q	1.234	1815.9	14.15	1.714	1.71	
	CCSD(T)/CA5	1.231	1830.2	13.91	1.720	1.73	0.101
	Experiment [38]	1.2333	1812.56	12.609	1.7151	1.708	
	Experiment [56]	1.2330	1813.2885	12.7779	1.7158		
NH^+ ($X^2\Pi$)	MRCI/CA5	1.068	3080.5	84.15	15.740	67.09	1.981[c]
	MRCI + Q	1.068	3077.4	84.17	15.730	67.06	
	CCSD(T)/CA5	1.068	3080.9	83.70	15.990	118.7	1.983[c]
	Experiment [38]	1.070	2922.0		15.35	64.0	
	Experiment [41]	1.0706					
NH ($A^3\Pi$)	MRCI/CA5	1.037	3270.0	122.21	16.48	47.74	1.232
	MRCI + Q	1.037	3267.2	122.13	16.48	48.18	
	CCSD(T)/CA5	1.036	3264.2	100.84	16.737	80.48	1.233
	Experiment [38]	1.03698	3231.2	98.6	16.6745	74.54	
NH ($c^1\Pi$)	MRCI/CA5	1.105	2372.4				1.629
	MRCI + Q	1.104	2366.1				
	Experiment [38]	1.1106	2122.64		14.537	59.3	
N_2^+ ($A^2\Pi$)	MRCI/aug-cc-pCV5Z	1.174	1915.6	16.87	1.746	1.83	0.0
	MRCI + Q	1.175	1906.7	16.96	1.743	1.84	
	CCSD(T)/cc-pCV5Z	1.173	1924.9	15.04	1.749	1.82	0.0
	Experiment [38]	1.1749	1903.70	15.02	1.7444	1.883	
NO ($X^2\Pi$)	MRCI/CA5	1.150	1919.0	15.52	1.707	1.74	0.194
	MRCI + Q	1.151	1909.4	15.49	1.703	1.75	
	CCSD(T)/CA5	1.150	1920.7	13.95	1.708	1.72	0.153
	Experiment [38]	1.15077	1904.204	14.075	1.67195	1.71	0.1587[d]
OH ($X^2\Pi$)	MRCI/CAQ	0.969	3786.9	99.46	18.924	71.68	1.628
	MRCI + Q	0.970	3780.5	99.82	18.907	71.99	
	CCSD(T)/cc-pCV5Z	0.969	3744.5	100.77	18.866	40.86	1.671
	Experiment [38]	0.96966	3737.761	84.8813	18.9108	72.42	1.6676(9)[e]
HCl^+ ($X^2\Pi$)	MRCI/CA5[f]	1.315	2714.5	60.44	9.955	31.78	1.691[c]
	MRCI/CA5[g]	1.312	2715.1	62.92	9.994	32.72	1.671[c]
	MRCI + Q[g]	1.313	2713.2	62.58	9.986	32.59	
	CCSD(T)/CAQ	1.314	2709.4	62.50	9.972	32.57	1.695[c]
	Experiment [38]	1.31468	2673.69	52.537	9.9566	32.71	
CCl ($X^2\Pi$)	MRCI/CA5	1.645	878.2	6.13	0.697	0.68	1.465
	MRCI + Q	1.645	881.0	6.12	0.697	0.68	
	CCSD(T)/CAQ	1.646	882.3	5.40	0.696	0.68	1.465[h]
	Experiment [38]	1.645	866.72	6.2	0.6936	0.672	
	Experiment [50]	1.6452					
OCl ($X^2\Pi$)	MRCI/CA5	1.565	871.1	6.32	0.627	0.59	1.366
	MRCI + Q	1.571	858.4	6.23	0.622	0.59	
	CCSD(T)/CAQ	1.570	861.6	6.06	0.623	0.59	1.327
	Experiment [38]	1.56963	853.8	5.5	0.623448	0.58	1.2974(10)[i]
NS ($X^2\Pi$)	MRCI/CA5	1.494	1216.4	7.60	0.775	0.63	1.720
	MRCI + Q	1.495	1219.3	7.63	0.775	0.63	
	CCSD(T)/CA5	1.492	1238.9	7.49	0.778	0.61	1.822
	Experiment [38]	1.49402	1218.7	7.28	0.775156	0.635	1.81(2)[j]
	Experiment [53]					0.6284[k]	

[a] CAX stands for the basis set including cc-pCVXZ and aug-cc-pVXZ (X = Q,5) sets assigned to the quadrupolar atom and the other atom, respectively.
[b] Freund et al. [8].
[c] In the center-of-mass system.
[d] Neumann [57], experimental value for the $v = 0$ level.
[e] Meerts and Dymanus [58].
[f] Based on CASSCF(9,10).
[g] Based on CASSCF(17,11).
[h] Woon and Herbst [59], RCCSD(T)/aug-cc-pVTZ gives $\mu = 1.404$ D, $R_e = 1.6577$ Å.
[i] Yaron [60], experimental value for the $v = 0$ level.
[j] Amano [61].
[k] Using the relation for the Dunham coefficient.

mined to be about three times smaller. A recent DFT calculation [6] at the experimental bond length was also not able to bring satisfactory agreement between the theoretical and experimental values. This discrepancy may be connected with the exceptionally large Λ-type doubling [37] probably caused by the interaction with the low-lying first excited $^2\Sigma^+$ state.

Table 3
^{14}N quadrupole coupling constants and electric dipole moments in $X^2\Pi$ ($^2\Pi_g$) states of selected triatomic species ABC.

ABC	eQq_0 (MHz)	eQq_2 (MHz)	μ (D)	Method	R_{AB} (Å)	R_{BC} (Å)	Source
CCN	−4.929	8.974	0.397	CASSCF(13,12)/icMRCI/CA5[a]	1.405[b]	1.189[b]	This work
	−5.235	8.958	0.441	CCSD(T)/CV5Z	1.405	1.189	This work
	−5.024	9.371	0.304	CASSCF(13,12)/icMRCI/CA5	1.383[c]	1.184[c]	This work
	−5.328	9.354	0.345	CCSD(T)/CA5	1.383	1.184	This work
	−5.160[d]	9.737[d]	0.425	MRD-CI/6s4p2d2f	1.405	1.189	[11]
	−4.8221(14)	9.208(66)		FIRLMR spectroscopy			[70]
NCO	−2.829	−16.688	0.756	CASSCF(15,12)/icMRCI/CA5	1.200[e]	1.206[e]	This work
	−2.809	−16.083	0.662	CCSD(T)/CA5	1.200	1.206	This work
	−2.190	−17.875	0.834	CASSCF(15,12)/icMRCI/CA5	1.232[c]	1.175[c]	This work
	−2.544	−17.254	0.737	CCSD(T)/CA5	1.232	1.175	This work
	−2.476	−17.206	0.722	CCSD(T)/CA5	1.237[f]	1.180[f]	This work
	−2.10	17.75	0.677	MRSD-CI/6s4p2d2f	1.237	1.180	[72]
	−2.211(12)[g]	−16.16(51)[g]	0.640(80)[h]	Microwave spectroscopy			[70] & cit.Ref.
N_3 (N^T)[i]	−0.029	−16.557		CASSCF(15,12)/icMRCI/cc-pCV5Z	1.184[j]	1.184	This work
(N^M)[i]	−0.752	−0.061					
N_3 (N^T)	−0.016	−15.963		CCSD(T)/cc-pCV5Z	1.184	1.184	This work
(N^M)	−0.712	−0.057					
N_3 (N^T)	−0.067	−16.569		CASSCF(15,12)/icMRCI/cc-pCV5Z	1.18115[k]	1.18115	This work
(N^M)	−0.770	−0.050					
N_3 (N^T)	0.029[l]	16.531[l]		MRD-CI-ino/6s4p2d2f	1.184	1.184	[77]
(N^M)	−0.831	−0.048					

[a] CA5 stands for the basis set including cc-pCV5Z and aug-cc-pV5Z sets assigned to the quadrupolar atom and the other atom, respectively.
[b] Prasad and Chandra [11], geometry optimization at the fv-(full-valence) CASSCF/6s4p2d2f level.
[c] Geometry optimization at the CCSD(T)/cc-pV5Z level.
[d] Q(^{14}N) = 0.02044 b used for the calculation of the NQCCs deduced from the EFG data of Ref. [11] using the formula (3b) of this paper.
[e] Misra et al. [71], experiment.
[f] Prasad [72]; geometry optimization at the fv-CASSCF/6s4p2d2f level.
[g] Values close to given NQCCs are presented in Ref.[73]: eQq_0 = −2.185(68) MHz and eQq_2 = 16.2(29) MHz.
[h] Saito and Amano [74], experiment.
[i] N^T denotes the terminal, N^M the middle atom.
[j] Prasad [75], geometry optimization at the fv-CASSCF/6s4p2d2f level.
[k] Brazier [77], R_0 bond length from experiment.
[l] For expressing NQCCs the value $Q(^{14}N)$ = 0.02044 b was used instead of 0.0205 b used in Ref. [75] .

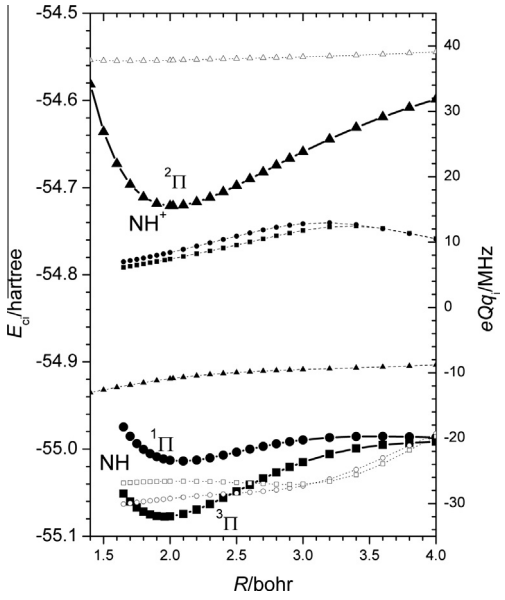

Fig. 1. R-dependences of total energy (large symbols), and ^{14}N quadrupole coupling constants eQq_0 (small solid symbols) and eQq_2 (small open symbols) corresponding to the $^2\Pi$ [NH^+] (triangle), $^1\Pi$ [NH] (circle) and $^3\Pi$ [NH] (square) electronic states as calculated by the icMRCI method (cf. Table 1).

With a slightly different geometry and basis set, the present calculation of the ^{14}N quadrupole coupling in NO ($X^2\Pi$) reproduces the outcome of Ref. [12]. It concerns a reasonable agreement between the theoretical and experimental values of both coupling constants, except a fine distinction in the vibrational dependence of eQ_Nq_2. While the magnitude of the experimentally determined eQ_Nq_2 for the vibrational $v = 1$ state is smaller compared to the vibrational ground state, the theoretical EFG curve passes a maximum at $v = 2$ before turning to a decline with $v > 2$. NO is an example of a molecule where the perpendicular electric quadrupole interaction represents, besides the magnetic Fermi-contact interaction, the dominant contribution to the hyperfine structure in its microwave spectra [45].

Concerning the diatomic molecules containing third-row elements, the agreement between the experimental and theoretical values of axial and perpendicular ^{35}Cl NQCCs in the $X^2\Pi$ states of OCl and CCl is reasonable. For these diatomics the leading electron configurations .. $(7\sigma)^2..(3\pi)^3$ and $..(7\sigma)^2..(3\pi)^1$ appear in the icMRCI wave functions at the equilibrium internuclear distance with about equal reference coefficients (∼0.94).

On the other hand NS ($X^2\Pi$), which is isoelectronic with CCl, shows no resemblance between the experimental and theoretical values of eQ_Nq_2, despite a fair agreement between the eQ_Nq_0 values, and an excellent agreement in the experimental and theoretical spectroscopic constants (cf. Table 2). Noticeable is the difference in the wave function representation of the two isoelectronic species. The NS ($X^2\Pi$) icMRCI wave function is characterized by the leading configuration with $c_0 \sim 0.92$ and further eight electron configurations with coefficients larger than 0.05, mainly based on different occupations of Hartree–Fock π orbitals; this number of configurations is about twice as much as that in the icMRCI wave functions of CCl and OCl. This result complies with the coupled-cluster T_1 diagnostic [23,24] for CCl and NS, yielding values 0.008 and 0.020, respectively. Despite significant multireference effects

in the electronic ground state of NS, both CCSD(T) and icMRCI methods applied to NS gave similar results concerning the ^{14}N quadrupole coupling. The change of the AS or/and basis set in the calculations did not lead to a significant improvement of eQ_Nq_2 for NS with respect to the experimental value. However, there still may be an open way for achieving more adequate values for the NQCCs [64], e.g., extrapolation to the complete basis set limit, extent of high-order effects in the electron correlation treatment and/or including relativistic effects. Interestingly, the experimental data from various authors [54,55] show also a significant variance in the eQ_Nq_2 values and wide error bars on the experimental values. We also used the icMRCI approach defined in Table 1 for evaluation of the ^{33}S nuclear quadrupole coupling in NS at R_e = 1.494 Å: our constants eQq_0 = 0.14 MHz and eQq_2 = −109.42 MHz comply with the rough estimate of Saleck et al. [53] 0.5(86) MHz and −61(73) MHz, respectively.

It is worth mentioning that the disagreement of the theoretical and experimental values cannot always be considered as a negative result. Sometimes it may corroborate [65] the refinement to a more accurate value, as it occurred with the experimental estimates of NQCCs for FNO in Refs. [66,67].

In order to give more evidence for the quantitative correctness of the correlated wave functions used for acquiring theoretical information on quadrupole coupling in diatomic molecules, spectroscopic constants were derived from the PEFs, collected in Table 2 and compared with available up-to-date experimental data. Within the icMRCI wave function expansion, the effect of higher excitations on the PEFs and corresponding spectroscopic constants has been assessed by the multireference analog of the Davidson correction [68,69], denoted by +Q. As expected, in the majority of cases the Davidson correction improves the agreement between the experimental and theoretical values. Optimized equilibrium structures and electric dipole moments of some molecules appearing in this paper were computed at the (fc)RCCSD(T)/aug-cc-pVXZ (X = T,Q,5) level and reported in a review article on properties of known and postulated neutral interstellar molecules by Woon and Herbst [59]. The corresponding values were used for comparison, if no experimental or other appropriate data were available.

Because the aim of the present calculations was primarily oriented on the nuclear quadrupole coupling, the outcome of our computations concerning spectroscopic constants does not necessarily reach the available most precise theoretical values approaching the experimental data. It concerns primarily the harmonic vibrational frequencies which can be unfavorably affected by applying different basis sets for the quadrupolar and nonquadrupolar atoms in a molecule.

In Table 3 our results on the ^{14}N electric quadrupole coupling constants as well as electric dipole moments concerning the radicals CCN, NCO and N_3 are compared with the available experimental and theoretical data. These three species belong into the class of non-hydride triatomic molecules with 16 valence electrons at most, and comply with the Walsh rules [76] assigning geometric linearity to their ground states. The major electronic configurations of CCN, NCO and N_3 in their equilibrium geometry comprise seven doubly occupied σ molecular orbitals and a group of π MOs $..(1\pi)^4(2\pi)^1$, $..(1\pi)^4(2\pi)^3$ and $..(\pi_u)^4(\pi_g)^3$, respectively. The leading configurations appear in the icMRCI wave function with very similar expansion coefficients ($c_0 \sim 0.90$), and the coupled-cluster T_1 diagnostic yields values of 0.024, 0.029 and 0.017, respectively. The parameters NQCCs and μ were calculated at equilibrium geometry which was taken from energy optimization processes of external and our own computations, and from experiment, if available. The optimization calculations of Woon and Herbst [59] at the (fc)CCSD(T)/aug-cc-pVTZ level gave for CCN and NCO geometries lying within the bond length values presented in Table 3 and dipole moments of 0.369 D and 0.715 D, respectively. The equilibrium geometries of the three radicals calculated by means of the symmetry-adapted–cluster configuration-interaction formalism [78] agree well with those presented in Table 3. A broader choice of geometries offers the possibility of not only confronting the theoretical and experimental data, but also assessing the variability of electric parameters with changes of the molecular geometry.

The theoretical electric hyperfine coupling constants and the dipole moments of the three radicals have been calculated earlier at various multiconfiguration SCF and multireference CI levels [11,72,75]. Table 3 shows that our application of different high-level many-electron methods using correlation-consistent and/or core-valence basis sets lead to similar results. In the case of N_3, for which there are no experimental data on the NQCCs, the quadrupole coupling parameters from both theoretical sources are well comparable. Concerning NCO, an opposing behavior of the calculated electric quadrupole coupling constants is observed, if two sets of equilibrium geometry are applied: switching from the estimated experimental geometry [71] to the optimized theoretical one brings about almost complete agreement in the theoretical eQ_Nq_0 with the experimental value, however a small deterioration in eQ_Nq_2.

The calculated ^{14}N nuclear quadrupole coupling constants of the largest Π-electron system treated in this paper, C_4N, are confronted in Table 4 with the data [79] derived from rotational spectra. C_4N is the second member of nitrogen-bearing carbon chain radicals, with the first member, C_2N, dealt with in Table 3. For this type of species it is characteristic that they have $^2\Pi$ ground states with well-resolved Λ-type doubling [79]. Tables 3 and 4 show that the electric dipole moment of C_4N is about three times smaller than the dipole moment of C_2N. As seen in Table 4, two sets of C_4N equilibrium geometry, based on energy optimization within the coupled-cluster models using the same basis set (aug-cc-pVTZ), were applied: The (fc)RCCSD(T) [59] (MOLPRO) and (all)CCSD(T) (ACES II) calculations yield slightly differing geometries which exercise no practical influence on the outcome of the calculated electric properties. Concerning the NQCCs, the icMRCI and CCSD(T) solutions

Table 4
^{14}N quadrupole coupling constants and electric dipole moment in the X $^2\Pi$ state of C_4N.

eQq_0 (MHz)	eQq_2 (MHz)	μ (D)	Method	R_{12} (Å)[a]	R_{23} (Å)	R_{34} (Å)	R_{45} (Å)
−4.393	4.525	0.133	CASSCF[b]/icMRCI[c]	1.337[d]	1.256	1.361	1.174
−4.369	4.286	0.039	CCSD(T)[c]	1.337	1.256	1.361	1.174
−4.455	4.723	0.174	CASSCF[b]/icMRCI[c]	1.327[e]	1.253	1.349	1.170
−4.433	4.461	0.096	CCSD(T)[c]	1.327	1.253	1.349	1.170
−4.429	4.453	0.080	CCSD(T)[f]	1.327	1.253	1.349	1.170
−4.389(1)	5.6(3)		FT MW spectry[79]				

[a] Numbering of the atoms: C^1–C^2–C^3–C^4–N^5.
[b] Occupation (12,4,4); closed (8,0,0).
[c] Basis set cc-pCVQZ for N, and cc-pVTZ for other atoms.
[d] Woon and Herbst[59], energy optimization at the RCCSD(T)/aug-cc-pVTZ level, μ = 0.060 D.
[e] Geometry optimization using CCSD(T)/aug-cc-pVTZ with ACES II.
[f] Basis set aug-cc-pCVQZ for N, and aug-cc-pVTZ for other atoms.

are in good accord despite the fact that the coupled-cluster T_1 diagnostic reaches the increased value of 0.028. From the two nuclear quadrupole coupling constants, the theoretical value of eQ_Nq_0 reproduces very well the value derived from the experiment.

4. Conclusions

The nuclear quadrupole coupling (NQC) in Π states of fifteen molecules consisting of 2 to 5 atoms has been investigated theoretically at high level of theory. The description of NQC in linear molecules with a spatially degenerate state requires two parameters, the axial (eQq_0) and perpendicular (eQq_2) NQCCs. The main purpose of the work was to bring further evidence that the originally one-electron (orbital) approach of Western et al. [10] to the calculation of eQq_2 is equally applicable if used in conjunction with many-electron wave functions. Two computational methods were used for obtaining both NQC parameters: an expectation value approach in association with the icMRCI method and a finite-field procedure, based on the single-configuration coupled-cluster model. In all calculations standard Dunning basis sets were designed to correlate core and valence electrons, and augmented with tight functions. With regard to experimental data, a semi-quantitative and sometimes good agreement was found for the eQq_0 NQCCs. For the eQq_2 parameters the situation is somewhat more complicated. The experimental eQq_2 data are frequently given with larger error bounds than the eQq_0 parameters, and in special cases the spectroscopic values from various authors differ significantly. Nevertheless, the agreement between theory and experiment is still acceptable. The calculated vibrational dependence of both NQCCs in diatomic molecules is in reasonable accord with the scarce experimental results. We believe that the theoretically determined eQq_2 parameters (in addition to eQq_0) can be useful for experimentalists in the analysis of the hyperfine structure in microwave spectra of molecules in Π-electronic states.

Acknowledgment

This study was supported by the Grant of the Ministry of Education of the Czech Republic (Grant No. MSM0021620857).

References

[1] W. Gordy, R.L. Cook, in: A. Weissberger (Ed.), Technique of Organic Chemistry, Part 2, Microwave Molecular Spectra, vol. 9, Interscience (Wiley), New York, 1970.
[2] P. Pyykkö, Mol. Phys. 106 (2008) 1965.
[3] J.N.P. Van Stralen, L. Visscher, Mol. Phys. 101 (2003) 2115.
[4] L. Demovič, V. Kellő, A.J. Sadlej, Chem. Phys. Lett. 498 (2010) 10.
[5] P.J. Bruna, F. Grein, J. Chem. Phys. 127 (2007) 074107.
[6] P.J. Bruna, F. Grein, J. Phys. Chem. A 113 (2009) 2615.
[7] K.F. Freed, J. Chem. Phys. 45 (1966) 4214.
[8] S.M. Freund, E. Herbst, R.P. Mariella Jr., W. Klemperer, J. Chem. Phys. 56 (1972) 1467.
[9] W. Ubachs, J.J. ter Meulen, A. Dymanus, Can. J. Phys. 62 (1984) 1374.
[10] C.M. Western, P.R.R. Langridge-Smith, B.J. Howard, S.E. Novick, Mol. Phys. 44 (1981) 145.
[11] R. Prasad, P. Chandra, J. Chem. Phys. 114 (2001) 1589.
[12] R. Polák, J. Fišer, Chem. Phys. 326 (2006) 611.
[13] H.-J. Werner, P.J. Knowles, J. Chem. Phys. 82 (1985) 5053.
[14] P.J. Knowles, H.-J. Werner, Chem. Phys. Lett. 115 (1985) 259.
[15] H.-J. Werner, P.J. Knowles, J. Chem. Phys. 89 (1988) 5803.
[16] P.J. Knowles, H.-J. Werner, Chem. Phys. Lett. 145 (1988) 514.
[17] MOLPRO, version 2010.1, a package of *ab initio* programs, H.-J. Werner, P.J. Knowles, F.R. Manby, M. Schütz, P. Celani, G. Knizia, T. Korona, R. Lindh, A. Mitrushenkov, G. Rauhut, T.B. Adler, R.D. Amos, A. Bernhardsson, A. Berning, D.L. Cooper, M.J.O. Deegan, A.J. Dobbyn, F. Eckert, E. Goll, C. Hampel, A. Hesselmann, G. Hetzer, T. Hrenar, G. Jansen, C. Köppl, Y. Liu, A.W. Lloyd, R.A. Mata, A.J. May, S.J. McNicholas, W. Meyer, M.E. Mura, A. Nicklaß, P. Palmieri, K. Pflüger, R. Pitzer, M. Reiher, T. Shiozaki, H. Stoll, A.J. Stone, R. Tarroni, T. Thorsteinsson, M. Wang, A. Wolf, see http://www.molpro.net.
[18] K. Raghavachari, G.W. Trucks, J.A. Pople, M. Head-Gordon, Chem. Phys. Lett. 157 (1989) 479.
[19] M.J.O. Deegan, P.J. Knowles, Chem. Phys. Lett. 227 (1994) 321.
[20] P.J. Knowles, C. Hampel, H.-J. Werner, J. Chem. Phys. 99 (1993) 5219; Erratum, J. Chem. Phys. 112 (2000) 3106.
[21] J.D. Watts, J. Gauss, R.J. Bartlett, J. Chem. Phys. 98 (1993) 8718.
[22] ACES II, Mainz–Austin–Budapest version, a quantum-chemical program package for high-level calculations of energies and properties, J.F. Stanton, J. Gauss, J.D. Watts, P.G. Szalay, R.J. Bartlett with contributions from A.A. Auer, D.B. Bernholdt, O. Christiansen, M.E. Harding, M. Heckert, O. Heun, C. Huber, D. Jonsson, J. Jusélius, W.J. Lauderdale, T. Metzroth, C. Michauk, D.P. O'Neill, D.R. Price, K. Ruud, F. Schiffmann, M.E. Varner, J. Vázquez. Integral packages included are MOLECULE (J. Almlöf, P.R. Taylor), PROPS (P.R. Taylor), and ABACUS (T. Helgaker, H.J. Aa. Jensen, P. Jørgensen, J. Olsen).
[23] T.J. Lee, J.E. Rice, G.E. Scuseria, H.F. Schaefer III, Theor. Chim. Acta 75 (1989) 81.
[24] T.J. Lee, Chem. Phys. Lett. 372 (2003) 362.
[25] H.D. Cohen, C.C.J. Roothaan, J. Chem. Phys. 43 (1965) S34.
[26] G.H.F. Diercksen, B.O. Roos, A.J. Sadlej, Chem. Phys. 59 (1981) 29.
[27] P.L. Cummins, G.B. Bacskay, N.S. Hush, R. Ahlrichs, J. Chem. Phys. 86 (1987) 6908.
[28] R. Polák, J. Fišer, Spectrochim. Acta A 58 (2002) 2029.
[29] R. Polák, J. Fišer, Chem. Phys. 290 (2003) 177.
[30] R. Polák, J. Fišer, Chem. Phys. 303 (2004) 73.
[31] R.A. Kendall, T.H. Dunning Jr, R.J. Harrison, J. Chem. Phys. 96 (1992) 6796.
[32] D.E. Woon, T.H. Dunning Jr, J. Chem. Phys. 100 (1994) 2975.
[33] D.E. Woon, T.H. Dunning Jr, J. Chem. Phys. 103 (1995) 4572.
[34] A. Halkier, H. Koch, O. Christiansen, P. Jørgensen, T. Helgaker, J. Chem. Phys. 107 (1997) 849.
[35] C. Puzzarini, A. Gambi, G. Cazzoli, J. Mol. Struct. 695–696 (2004) 203.
[36] MOLCAS-4, a package of ab initio programs, K. Andersson, M.R.A. Blomberg, M.P. Fülscher, G. Karlström, R. Lindh, P.-Å. Malmqvist, P. Neogrády, J. Olsen, B.O. Roos, A.J. Sadlej, M. Schütz, L. Seijo, L. Serrano-Andrés, P.E.M. Siegbahn, P.-O. Widmark, Lund University, Sweden, 1997.
[37] C. Yamada, M. Fujitake, E. Hirota, J. Chem. Phys. 91 (1989) 137.
[38] K.P. Huber, G. Herzberg, Molecular Spectra and Molecular Structure. IV. Constants of Diatomic Molecules, Van Nostrand, New York, 1979.
[39] M.L. Hause, G.E. Hall, T.J. Sears, J. Mol. Spectrosc. 253 (2009) 122.
[40] P. Verhoeve, J.J. ter Meulen, W.L. Meerts, A. Dymanus, Chem. Phys. Lett. 132 (1986) 213.
[41] H.-W. Hübers, K.M. Evenson, Ch. Hill, J.M. Brown, J. Chem. Phys. 131 (2009) 034311.
[42] W. Ubachs, G. Meyer, J.J. ter Meulen, A. Dymanus, J. Mol. Spectrosc. 115 (1986) 88.
[43] P.J. Bruna, F. Grein, J. Mol. Spectrosc. 250 (2008) 75.
[44] R.S. Lowe, A.R.W. McKellar, P. Veillette, W.L. Meerts, J. Mol. Spectrosc. 88 (1981) 372.
[45] E. Klisch, S.P. Belov, R. Schieder, G. Winnewisser, Mol. Phys. 97 (1999) 65.
[46] K.R. Leopold, K.M. Evenson, E.R. Comben, J.M. Brown, J. Mol. Spectrosc. 122 (1987) 440.
[47] K.G. Lubic, D. Ray, D.C. Hovde, L. Veseth, R.J. Saykally, J. Mol. Spectrosc. 134 (1989) 1.
[48] H. Gupta, B.J. Drouin, J.C. Pearson, Astrophys. J. Lett. 751 (2012) L38.
[49] P.J. Bruna, F. Grein, Mol. Phys. 104 (2006) 429.
[50] Y. Endo, S. Saito, E. Hirota, J. Mol. Spectrosc. 94 (1982) 199.
[51] R.K. Kakar, E.A. Cohen, M. Geller, J. Mol. Spectrosc. 70 (1978) 243.
[52] E.A. Cohen, H.M. Pickett, M. Geller, J. Mol. Spectrosc. 106 (1984) 430.
[53] A.H. Saleck, H. Ozeki, S. Saito, Chem. Phys. Lett. 244 (1995) 199.
[54] S.K. Lee, H. Ozeki, S. Saito, Astroph. J. Suppl. Ser. 98 (1995) 351.
[55] J.R. Anacona, M. Bogey, P.B. Davies, C. Demuynck, J.L. Destombes, Mol. Phys. 59 (1986) 81.
[56] R.S. Ram, L. Wallace, P.F. Bernath, J. Mol. Spectrosc. 263 (2010) 82.
[57] R.M. Neumann, Astrophys. J. 161 (1970) 779.
[58] W.L. Meerts, A. Dymanus, Chem. Phys. Lett. 23 (1973) 45.
[59] D.E. Woon, E. Herbst, Astrophys. J. Suppl. Ser. 185 (2009) 273.
[60] D. Yaron, K. Peterson, W. Klemperer, J. Chem. Phys. 88 (1988) 4702.
[61] T. Amano, S. Saito, E. Hirota, Y. Morino, J. Mol. Spectrosc. 32 (1969) 97.
[62] R. Polák, J. Fišer, J. Mol. Struct. (Theochem.) 584 (2002) 69 [Erratum, J. Mol. Struct. (Theochem.) 589–590 (2002) 465].
[63] R. Polák, J. Fišer, Collect. Czech. Chem. Commun. 68 (2003) 509.
[64] C. Puzzarini, V. Barone, J. Chem. Phys. 133 (2010) 184301.
[65] R. Polák, J. Fišer, Chem. Phys. 351 (2008) 83.
[66] K.S. Buckton, A.C. Legon, D.J. Millen, Trans. Faraday Soc. 65 (1969) 1975.
[67] C. Styger, B. Gatehouse, N. Heineking, W. Jäger, M.C.L. Gerry, J. Chem. Soc. Faraday Trans. 89 (1993) 1899.
[68] S.R. Langhoff, E.R. Davidson, Int. J. Quantum Chem. 8 (1974) 61.
[69] M.R.A. Blomberg, P.E.M. Siegbahn, J. Chem. Phys. 78 (1983) 5682.
[70] M.D. Allen, K.M. Evenson, D.A. Gillett, J.M. Brown, J. Mol. Spectrosc. 201 (2000) 18.
[71] P. Misra, C.W. Mathews, D.A. Ramsay, J. Mol. Spectrosc. 130 (1988) 419.
[72] R. Prasad, J. Chem. Phys. 120 (2004) 10089.
[73] K. Kawaguchi, S. Saito, E. Hirota, Mol. Phys. 55 (1985) 341.
[74] S. Saito, T. Amano, J. Mol. Spectrosc. 34 (1970) 383.
[75] R. Prasad, J. Chem. Phys. 119 (2003) 9549.
[76] A.D. Walsh, J. Chem. Soc. (1953) 2266.
[77] C.R. Brazier, P.F. Bernath, J.B. Burkholder, C.J. Howard, J. Chem. Phys. 89 (1988) 1762.
[78] M. Ehara, J.R. Gour, P. Piecuch, Mol. Phys. 107 (2009) 871.
[79] M.C. McCarthy, G.W. Fuchs, J. Kucera, G. Winnewisser, P. Thaddeus, J. Chem. Phys. 118 (2003) 3549.